Robust Waterflooding Optimization of Multiple Geological Scenarios

G.M. van Essen, SPE, **M.J. Zandvliet,** SPE, **P.M.J. Van den Hof,** and **O.H. Bosgra,** Delft University of Technology; and **J.D. Jansen,** SPE, Delft University of Technology and Shell International E&P

Summary

Dynamic optimization of waterflooding using optimal control theory has significant potential to increase ultimate recovery, as has been shown in various studies. However, optimal control strategies often lack robustness to geological uncertainties. We present an approach to reduce the effect of geological uncertainties in the field-development phase known as robust optimization (RO). RO uses a set of realizations that reflect the range of possible geological structures honoring the statistics of the geological uncertainties. In our study, we used 100 realizations of a 3D reservoir in a fluvial depositional environment with known main-flow direction. We optimized the rates of the eight injection and four production wells over the life of the reservoir, with the objective to maximize the average net present value (NPV). We used a gradient-based optimization method in which the gradients are obtained with an adjoint formulation. We compared the results of the RO procedure to two alternative approaches: a nominal-optimization (NO) and a reactive-control approach. In the reactive approach, each production well is shut in when production is no longer profitable. The NO procedure is based on a single realization. In our study, the NO procedure is performed on each of the 100 realizations in the set individually, resulting in 100 different NO-production strategies. The control strategies were applied to each realization, from which the average NPVs, the standard deviation, the cumulative-distribution functions, and the probability-density functions were determined. The RO results displayed a much smaller variance than the alternatives, indicating an increased robustness to geological uncertainty. Moreover, the RO procedure significantly improved the expected NPV compared to the alternative methods (on average 9.5% higher than using reactive-control and 5.9% higher than the average of the NO strategies).

Introduction

In this paper, we consider the secondary-recovery phase of a petroleum reservoir using waterflooding. In this case, a number of injection and production wells are drilled to preserve a steady reservoir pressure and sweep the reservoir. The use of smart wells expands the possibilities to manipulate and control fluid-flow paths through the oil reservoir. The ability to manipulate (to some degree) the progression of the oil/water front provides the possibility to search for a control strategy that will result in maximization of ultimate oil recovery.

Dynamic optimization of waterflooding using optimal control theory has significant potential to increase ultimate recovery by delaying water breakthrough and increasing sweep, as has been shown in various studies (Brouwer and Jansen 2004). However, optimal control strategies often lack robustness to geological uncertainties. By discarding these uncertainties, the sensitivity to a possibly large system/model mismatch is not taken into account within the optimization procedure. As a result, the optimal control strategy may cease to be optimal or may even result in very poor performance.

Dealing with uncertainty is a topic encountered in many fields related to modeling and control. It can essentially be divided into two different strategies, which are not mutually exclusive: reducing the uncertainty itself using measurements [i.e., history matching (Landa and Horne 1997, Li et al. 2003)] and reducing the sensitivity to the uncertainty. In this paper, we consider a situation in which no production data are assumed to be available, which rules out any history-matching approach to reduce the geological uncertainty. Our study forms part of a larger research project to enable closed-loop, model-based reservoir management (Jansen et al. 2005).

A suggested approach from the process industry, to optimization problems that suffer from vast uncertainty and limited measurement information, is the use of a so-called RO technique (Srinivasan et al. 2003, Terwiesch et al. 1998, Ruppen et al. 1995). In RO, the optimization procedure is performed over a set of realizations, actively accounting for the influence of the uncertainty. The implementation of multiple realizations within the optimization process has been addressed by Yeten et al. (2002). However, their study deviates in the way the realizations are incorporated in the objective function, in the optimization method, and in the number of realizations. The goal of our paper is to present an RO procedure on the basis of a set of 100 realizations of a 3D oil/water reservoir, which leads to a control strategy that accounts explicitly for geological uncertainty.

Theory

Optimal Control. We consider an optimal control problem in which the injection-flow rates and production-flow rates are manipulated directly (i.e., a rate-constrained scenario). The objective is to maximize the simple NPV of the cumulative oil and water production over a fixed time horizon. The objective function (or cost function) is thus given by (Brouwer and Jansen 2004)

$$J(\mathbf{q}_{1:K}) = \sum_{k=1}^{K} J_k(\mathbf{q}_{1:k}) = \sum_{k=1}^{K} \frac{\Delta t_k \left[-r_o \cdot q_{o,k}(\mathbf{q}_{1:k}) + r_{wp} \cdot q_{wp,k}(\mathbf{q}_{1:k}) - r_{wi} \cdot q_{wi,k} \right]}{(1+b_\tau)^{\frac{t_k}{\tau}}}, \quad \ldots\ldots(1)$$

where r_o is the oil revenue, r_{wp} is the water-production cost, and r_{wi} is the water-injection cost, which are all assumed positive and constant. The variable $q_{o,k}$ represents the total flow rate (i.e., summed over all wells) of produced oil, $q_{wp,k}$ is the total flow rate of produced water, and $q_{wi,k}$ is the total flow rate of injected water, at discrete time k. We use the convention that injection rates are positive and production rates negative, such that the oil revenues in the objective function Eq. 1 are positive and the costs negative. The variable K represents the total number of timesteps k, Δt_k the time interval of timestep k, and t_k is the cumulative time until k. The variable $\mathbf{q}_k$ is a vector of the liquid-flow rates in all wells, which act as the control variables (input variables) in our optimization problem, at discrete time k. The colon in the subscript is used to indicate a sequence (i.e., $\mathbf{q}_{1:K}$ implies $q_k, k = 1, \ldots, K$). The oil- and water-production rates $q_{o,k}$ and $q_{wp,k}$ at discrete time k are functions of the total flow rates $\mathbf{q}_k$ through their dependence on the (saturation-dependent) fractional flow in the well gridblocks. The saturations are, in turn, functions of the current and all previous inputs $\mathbf{q}_{1:k}$, such that $q_{o,k}$ and $q_{wp,k}$ become complex functions of $\mathbf{q}_{1:k}$. The parameter b in the denominator of Eq. 1 is the discount rate per time unit τ and is considered to be equal to zero in this paper. The optimization problem involves finding the optimal injection- and production-flow rates $\mathbf{q}_{1:k}$ that maximize the performance measure $J(\mathbf{q}_{1:K})$, while honoring the dynamic system

This paper (SPE 102913) was accepted for presentation at the SPE Annual Technical Conference and Exhibition, San Antonio, Texas, 24–27 September 2006, and revised for publication. Original manuscript received for review 22 June 2006. Revised manuscript received for review 14 March 2008. Paper peer approved 27 August 2008.

equations. We use a gradient-based optimization algorithm to converge to the (possibly locally) optimal flow rates. The gradients are the transposes of the derivatives (i.e., $\nabla J_k = (\mathrm{d}J/\mathrm{d}\mathbf{q}_k)^T$, and the derivatives

$$\frac{\mathrm{d}J}{\mathrm{d}\mathbf{q}_k} = \sum_{\kappa=k}^{K} \frac{\partial J_\kappa}{\partial \mathbf{q}_k}, k = 1, \ldots, K \quad \ldots\ldots\ldots\ldots\ldots\ldots\ldots\ldots\ldots\ldots (2)$$

are obtained by solving a system of adjoint equations as described by, for example, Brouwer and Jansen (2004) and Sarma et al. (2005). (See Appendix A for a brief description of the adjoint-based method to obtain the gradient information.) The gradients are used in a steepest ascent (SA) algorithm to iteratively converge to the optimal input trajectory:

$$\mathbf{q}_k^{i+1} = \mathbf{q}_k^i + \alpha \left(\frac{\mathrm{d}J}{\mathrm{d}\mathbf{q}_k} \right)^T, k = 1, \ldots, K, \quad \ldots\ldots\ldots\ldots\ldots\ldots\ldots\ldots (3)$$

where α is the step size of the algorithm and i is the iteration counter. A line search to find the optimal step size along the direction of the greatest ascent could be used to speed up the iterative procedure, but because our study was not aimed at improving convergence speed, we used a fixed α for simplicity's sake.

Using Eq. 3, a situation may occur in which the new flow rates $\mathbf{q}_k^{i+1}, k = 1, \ldots K$ do not obey the constraint equations as addressed in more detail in Eqs. A-7 and A-8 in Appendix A. To ensure that they comply with the constraints, feasible search directions $\mathbf{d}_k$ of the gradient vectors $(\mathrm{d}J/\mathrm{d}\mathbf{q}_k)^T$ need to be determined. Sarma et al. (2006) proposed an effective but rather complicated method to obtain feasible directions if there are state constraints. De Montleau et al. (2006) and Kraaijevanger et al. (2007) also discuss production optimization under state constraints. However, because we are dealing with linear equality and inequality constraints on the input variables only, we can simply apply the gradient projection method as described in Luenberger (1984) to determine $\mathbf{d}_k$. Using $\mathbf{d}_k$, the SA algorithm thus becomes

$$\mathbf{q}_k^{i+1} = \mathbf{q}_k^i + \alpha \mathbf{d}_k. \quad \ldots\ldots\ldots\ldots\ldots\ldots\ldots\ldots\ldots\ldots\ldots\ldots\ldots\ldots (4)$$

Determining a feasible search direction $\mathbf{d}_k$, however, still does not guarantee that $\mathbf{q}_k^{i+1}$ is feasible, given the fixed step size α. It merely ensures that a certain $\alpha > 0$ exists for which it is feasible. For this reason, after $\mathbf{d}_k$ is determined, it is subsequently checked for its feasibility. If the result of this check is negative, α is scaled down until a feasible $\mathbf{q}_k^{i+1}$ is reached. Reducing the step size slows down the convergence rate of the SA method. However, we note that checking if feasibility of the input (flow rates) is violated and subsequently finding a reduced step size that ensures feasibility does not require any additional simulation runs.

Geological Scenarios. The need to model uncertainty is an inevitable result of the modeling process itself; it is simply impractical or impossible to capture all dynamics and properties of a real dynamical system. Often, adopting an "uncertain" model description in a model-based control scheme does not create problems. The modeling error may be small, and output and measurement data can be used to correct the predicted state and parameter values to their real values.

Unfortunately, this does not hold for control strategies based on reservoir models. The geological uncertainty is generally profound because of the noisy and sparse nature of seismic data, core samples, and borehole logs. Besides, during production, this uncertainty can be reduced only marginally because the measurement and output data provide only limited information on the true values of the (large number of) states and model parameters.

The consequence of a large number of uncertain model parameters ($\boldsymbol{\theta}$) is the broad range of possible models that may satisfy the seismic and core-sample data. Nevertheless, in many cases, for reasons of simplicity, a single reservoir model is adopted in which the uncertain parameters $\boldsymbol{\theta}$ are converted to deterministic parameters $\boldsymbol{\eta}$ by taking their expected values (i.e., $\boldsymbol{\eta} := E[\boldsymbol{\theta}]$). However, because we are looking at the NPV (denoted by J) as a measure of performance, we are far more interested in the expected *NPV* over the uncertainty space Θ (spanned by the uncertain parameters $\boldsymbol{\theta}$). It should be noted that this is generally not the same as taking the expected value of the uncertain parameters:

$$E_\theta[J(\mathbf{q}_{1:K}, \theta)] \neq J(\mathbf{q}_{1:K}, E_\theta[\theta]), \theta \in \Theta. \quad \ldots\ldots\ldots\ldots\ldots\ldots (5)$$

A better approximation of the expected NPV may be obtained by discretizing the uncertainty space Θ, resulting in a finite number (N_r) of realizations of $\boldsymbol{\theta}$, and calculating the expected value over the discretized uncertainty space:

$$E_\theta[J(\mathbf{q}_{1:K}, \theta)] \approx$$
$$E_{\theta_d}[J(\mathbf{q}_{1:K}, \theta_d)], \theta_d := \{\theta_1, \ldots, \theta_{N_r}\}, \quad \ldots\ldots\ldots\ldots\ldots\ldots (6)$$

where $\boldsymbol{\theta}_d$ is the finite set of (deterministic) realizations of $\boldsymbol{\theta}$. In the special case that the realizations are equiprobable, the right-hand side of Eq. 6 is simply the average of the Js, given by:

$$E_{\theta_d}[J(\mathbf{q}_{1:K}, \theta_d)] = \frac{1}{N_r} \sum_{i=1}^{N_r} J(\mathbf{q}_{1:K}, \theta_i). \quad \ldots\ldots\ldots\ldots\ldots\ldots (7)$$

If the realizations are not equiprobable, a weighted average of the Js can be used, by applying different weighting factors to the Js resulting from each realization. If we assume that the modeling uncertainty is limited to uncertainty caused by a lack of information on the true geological structure of the reservoir, the realizations of $\boldsymbol{\theta}$ are usually referred to as geological scenarios. Several methods are available to create an ensemble of geological scenarios. A geologist may create a number of scenarios based on his own knowledge and experience with comparable reservoirs. The uncertainty space thus provides the geologist with the boundaries within which he/she can design possible realizations. The advantage of such a method is that geological realism of the scenarios is guaranteed. It is, however, a rather subjective process; therefore, the set may be biased. A geostatistics-based method, such as multiple-point geostatistics (Strebelle 2000, Caers et al. 2003), incorporates statistical information on geological parameters and, consequently, does not suffer from this problem. It is, however, more difficult to generate geologically realistic structures in this manner. Alternatively, geological realizations may be created with object-based or process-based algorithms, which usually produce realistic geological structures but are difficult to condition to well data (Deutsch and Tran 2002, Viseur 1999, Thomas and Nicholas 2002, Gross and Small 1998).

RO. The use of an ensemble of geological scenarios to determine the expected revenues from a reservoir given a specified production strategy is not uncommon. Implementing such an ensemble in an optimization scheme has, however, not found its way into oil-recovery-optimization methods yet. Using a set of realizations to account for the effect of uncertainty within optimization problems, which suffer from uncertainty and limited measurement information, is not uncommon in the downstream petroleum industry. These optimization procedures are referred to as RO techniques. Within RO, the set of realizations may be used in various ways to account for the effect of uncertainty. These different approaches are represented by RO objectives (Srinivasan et al. 2003, Terwiesch et al. 1998, Ruppen et al. 1995). The most straightforward RO objective is using the expected outcome over the set of realizations, which is, in our case, equivalent to Eq. 7. Other objectives may involve incorporating the variance of the outcomes or a worst-case approach. In this work, however, we limit ourselves to the expected NPV, represented by the robust objective function J_{rob}.

$$J_{\mathrm{rob}}(\mathbf{q}_{1:K}) = \frac{1}{N_r} \sum_{i=1}^{N_r} J(\mathbf{q}_{1:K}, \theta_i). \quad \ldots\ldots\ldots\ldots\ldots\ldots\ldots\ldots (8)$$

This results in the following RO problem:

$$\max_{\mathbf{q}_{1:K}} J_{\mathrm{rob}}(\mathbf{q}_{1:K}). \quad \ldots\ldots\ldots\ldots\ldots\ldots\ldots\ldots\ldots\ldots\ldots\ldots (9)$$

TABLE 1—GEOLOGICAL AND FLUID PROPERTIES EXAMPLE		
Property	Value	Units
ϕ	0.20	–
ρ_o (at 1 bar)	1000	kg/m^3
ρ_w (at 1 bar)	1000	kg/m^3
c_o	10^{-5}	1/bar
c_w	10^{-5}	1/bar
μ_o	10^{-3}	Pa·s
μ_w	10^{-3}	Pa·s
p_{cow}	0	bar

From this formulation, it follows that calculating the expected NPV (i.e., the value of J_{rob}) involves a linear operation. As a result, calculating the gradients of Eq. 9 involves a linear operation in terms of the gradients of each realization.

$$\frac{\mathrm{d}J_{\text{rob}}}{\mathrm{d}\mathbf{q}_k} = \frac{1}{N_r}\sum_{i=1}^{N_r}\frac{\mathrm{d}J(\mathbf{q}_{1:K},\theta_i)}{\mathrm{d}\mathbf{q}_k}. \quad \ldots\ldots\ldots\ldots\ldots\ldots\ldots\ldots\ldots\ldots\ldots\ldots(10)$$

The fact that calculating the mean gradients $(\mathrm{d}J_{\text{rob}}/\mathrm{d}\mathbf{q}_k)^T$ involves a linear operation has the advantage that the gradients of each realization can be determined separately. As a result, the gradients can be calculated sequentially instead of simultaneously, which would result in a considerable computational burden, limiting the number of realizations to be used. Calculating the gradients sequentially solves this problem, but it does lead to an extended simulation time by a factor N_r. However, the fact that the calculations are decoupled allows for parallel calculations on multiple processors.

Example

We considered a waterflooding example of a 3D oil/water-reservoir model containing eight injection wells and four production wells. Production from the reservoir was simulated over a time horizon of 10 years, with timesteps of $^1/_{16}$ year. The model contains 18,553 gridblocks $8\times8\times4$m in size, and there are seven vertical layers. The average reservoir pressure was set at 400 bar, and the initial water saturation was taken to be uniform over the reservoir at a value of 0.1. The remaining geological and fluid properties used in this example are presented in **Table 1.** The reservoir is located in a fluvial depositional environment with known main-flow direction. Seismic and core-sample data from appraisal wells were assumed to provide no specific knowledge on the meandering structure of the fluvial depositions. In this example, the lack of information about the real geological structure was assumed to be the only contributor to the modeling uncertainty.

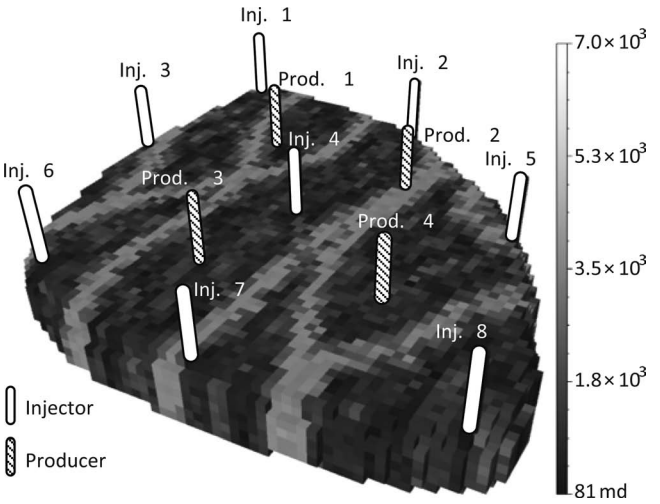

Fig. 1—Permeability field and well locations of Realization Number 1 of a set of 100 realizations.

Two different sets of 100 geological realizations of the reservoir were generated, based on geological insight rather than a geostatistical method. In other words, the geologist sketched them by hand. Although it may be argued that a more sophisticated method is to be preferred in practice, the method of creating realizations is unrelated to the optimization strategy presented in this paper. Each set of realizations represents the range of possible geological structures within the boundaries of the geological uncertainties. The number of 100 realizations is assumed to be large enough to be a good representation of this range. To check whether this is a reasonable assumption, the responses of the two sets to identical control strategies were compared. It should be noted that similar responses (in a statistical sense) indicate that this assumption is plausible, but do not provide a conclusive validation. The manual method by which the different realizations were created does not give a classification between the members in the set. No information from seismic, production, or other data was assumed to be available to rank the realizations; therefore, they were assumed to be equiprobable.

The absolute-permeability field and well locations of the first realization of the set are depicted in **Fig. 1. Fig. 2** displays the absolute-permeability field of six realizations randomly selected from the set without the wells. The minimum rate for each well was chosen equal to 0.02 m^3/d because setting the rate equal to 0 m^3/d presented numerical problems when solving the system of adjoint equations. The maximum rate for each well was fixed at 64 m^3/d. To keep the reservoir pressure constant, the total injection rate must be equal to the total production rate at each time instant.

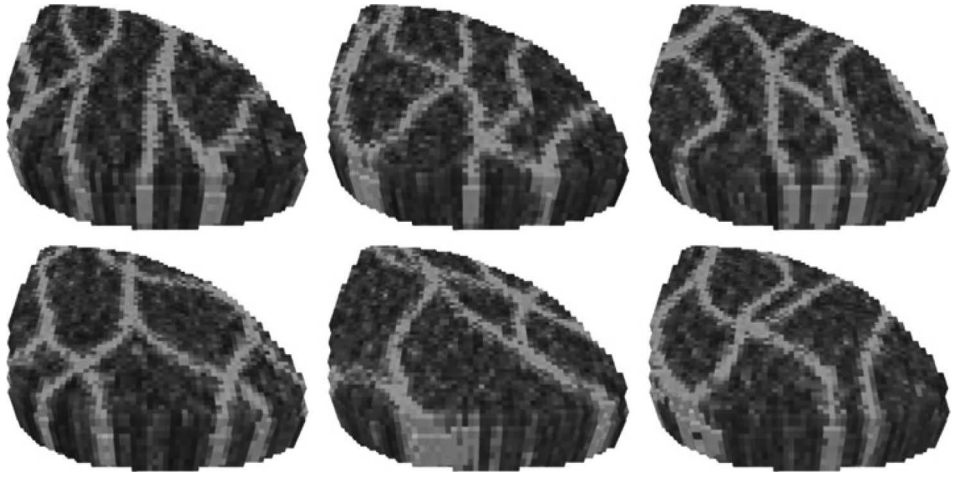

Fig. 2—Permeability field of six (randomly chosen) realizations out of a set of 100, showing alternative fluvial structures.

Production Strategies. We considered three production strategies: a reactive approach, an NO approach, and an RO approach. Their performances were evaluated using the objective function as defined in Eq. 1, with r_o = USD 126 /m^3, r_w = USD 19 /m^3, and r_i = USD 6 /m^3. However, because of the geological uncertainty, a deterministic estimate of performance cannot be given. Therefore, the performance of each of the three strategies was estimated in a probabilistic sense, using the set of 100 realizations. For each strategy, the 100 deterministic values of the objective function resulting from the set were used to determine a cumulative distribution function (CDF) and to estimate a probability density function (PDF).

Reactive Approach. Using the reactive approach, each production well is simply shut in if production is no longer profitable, where the profitability threshold corresponds to a water cut of 87%. The production-flow rates are initially fixed at their maximum capacity of 64 m^3/d. The injection-flow rates are equal for each injection well and are initially fixed at 32 m^3/d to honor the balanced injection and production. If a production well is shut in, the injection rate of each injection well is proportionally scaled down to meet the equality constraint, described in Appendix A by Eq. A-8. This reactive strategy will be used as a benchmark for the optimal control strategies that need predictive reservoir models to determine a strategy. The advantage of a reactive strategy is that it is model-free. Thus, when applied to an actual field, it does not suffer from a wrong representation of the geological realizations, whereas model-based methods do. However, the disadvantage is that it usually does not lead to an optimal reservoir flooding in terms of life-cycle performance. In the field-development phase of a project, we can assess the performance of a reactive strategy vs. a model-based strategy by simulating the performance of both strategies on a set of realizations. This assessment is valid only under the assumption that the set is a good representation of the true modeling uncertainty and, thus, can reflect the truth. If the used set is far from the truth, it is impossible to say which of the considered control strategies will perform better. We applied the reactive control strategy to each of the 100 members of the set of realizations. **Fig. 3** displays the response of the four production wells in terms of water cut over time for each of the 100 realizations. The large spread in water-breakthrough times gives an indication of the level of variability that the realizations are meant to represent. Note that the production wells are shut in when the profitability threshold of 87% water cut is reached. Applying the reactive control strategy to each of the 100 members also resulted in 100 values of the objective function (Eq. 1). The corresponding CDF and PDF, as depicted in **Fig. 4,** provide a probabilistic estimate of the performance of the reactive production strategy when applied to the true reservoir. The expected NPV and estimated standard deviation of the strategy are presented in **Table 2.**

NO. The NO approach is based on a single realization. However, because none of the realizations in the set of 100 is preferred over the others, the decision of which realization to use in the NO approach becomes an arbitrary one. To avoid the possibility of a biased choice, the NO procedure was performed on each of the 100 realizations in the set individually, resulting in 100 different NO production strategies. The number of control parameters for the optimization procedure is equal to the number of timesteps times the number of wells, which comes to 1,920 parameters. However, by using the adjoint method to obtain the gradients, the number of control parameters is not an issue because it requires only a single adjoint simulation to compute the gradients to all control parameters. The initial injection- and production-flow rates were set constant over time and equal to 24 m^3/d and 48 m^3/d, respectively. In the SA algorithm, a fixed step size t is used of 3×10^{-4}, which was chosen on the basis of a number of trial runs. The optimization was brought to an end after 80 iterations, at which point the incremental change of the objective function was less than 0.04% for all cases. The optimization procedure required a little more than 3 hours to converge to the optimal solution on a single computer for a single realization. Using a different optimization scheme or better constraint handling, we could have reached the convergence faster. However, improved convergence was not the goal of this study and was, therefore, not investigated further. The optimal injection- and production-flow rates resulting from the NO procedure based on

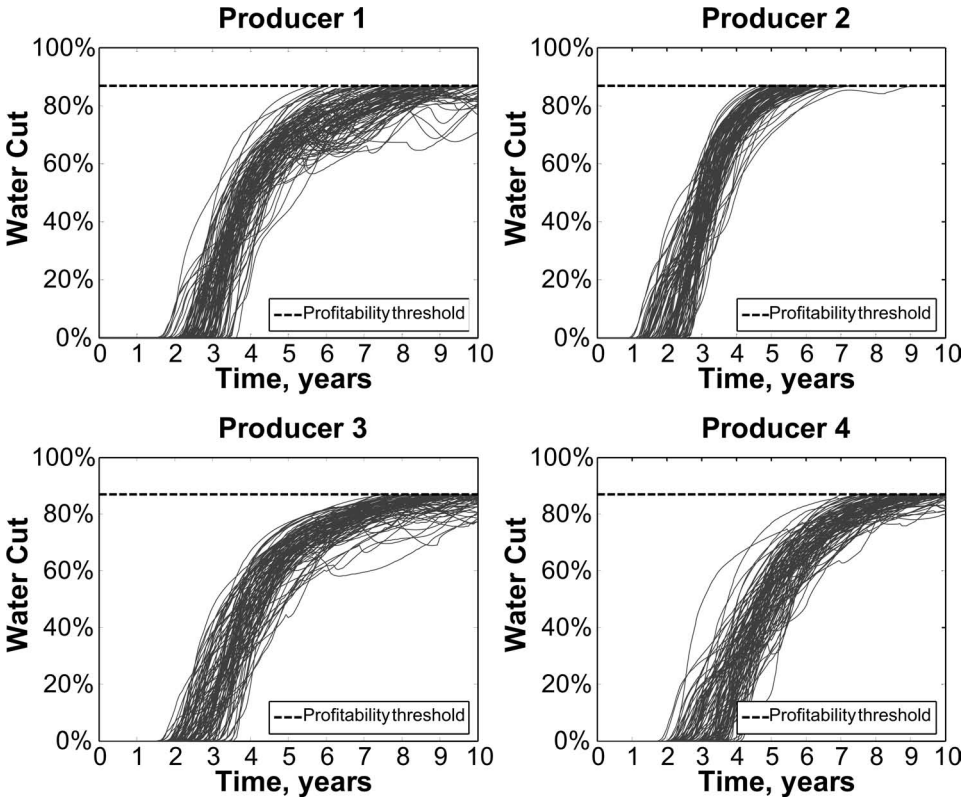

Fig. 3—Response of the four production wells to the reactive control strategy in terms of water cut over time for each of the 100 realizations. The production wells are shut in when the profitability threshold of 87% water cut is reached.

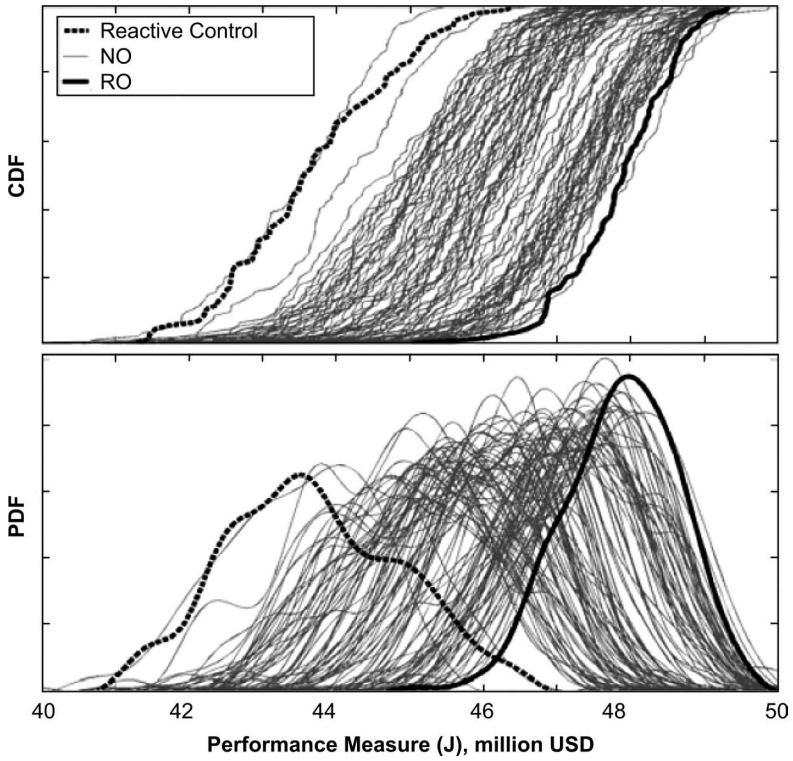

Fig. 4—CDF and PDF based on the first set of 100 realizations of the reactive control strategy, the 100 NO strategies, and the RO strategy.

Realization Number 1 have been displayed in **Fig. 5.** The performance of each of these 100 strategies on the entire ensemble was assessed by applying them to each member of the set. This resulted in 100 × 100 values of the objective function (Eq. 1), from which 100 CDFs and PDFs were determined, one for each strategy, as shown in Fig. 4. For each NO strategy, the expected NPV and the standard deviation were determined. The averages of these 100 expected NPV values and standard deviations are presented in Table 2.

RO. The RO approach uses the entire set of realizations to determine a control strategy that maximizes the expected NPV over the entire set of realizations. The robust optimal control strategy is determined using the same gradient-based optimization procedure and optimization parameters that were used in the NO approach. However, calculating the robust gradient information requires calculating the gradients for each realization individually. Hence, the simulation time is approximately 100 times longer than the time needed for the NO approach (i.e., approximately 2 weeks). The RO control strategy was again applied to each realization in the set, and the value of the objective function was determined for each member. The resulting CDF and PDF are depicted in Fig. 4, and the expected NPV and standard deviation are presented in Table 2.

Results

The first observation from Fig. 4 is that, given the set of realizations used in this example, a different choice of realization as a basis for the NO procedure can have a profound effect on the performance of the resulting NO strategy. A bad choice may lead to a drop of almost 10% in terms of expected NPV, compared to the expected NPV of a good choice.

A second observation from Fig. 4 is that, in this example, almost all NO control strategies perform better than the reactive control strategy. Table 2 shows that, on average, the expected NPV of the NO control strategies is 5.9% higher than the expected NPV of a reactive control strategy. Also, the standard deviation is, on average, smaller than that of the reactive approach. This indicates that the NO control strategies, on average, show an increased robustness to the effect of the considered geological uncertainty.

Fig. 4 and Table 2 show that the performance of the RO control strategy is greatly improved over the performance of the reactive control strategy. The expected NPV increases 9.5%. The standard deviation is also reduced considerably, although a reduction in variance is not part of the objective function (Eq. 1). On average, the performance of the RO strategy is also improved compared to the NO strategies. It performs better than 99 out of the 100 NO strategies, though the difference in the expected NPV of the best NO control strategy and the RO control strategy is very small. This may be the effect of an RO procedure that was not fully converged or of the RO strategy leading to a local optimum in expected NPV. This was not investigated further.

Finally, using the mean gradients $(\mathrm{d}J_{\mathrm{rob}}/\mathrm{d}\mathbf{q})^T$ in the RO procedure has a regularizing effect on the resulting control strategy, as can be seen in Fig. 5. The RO control strategy shows less-frequent and much smoother changes of the flow rates compared to the NO control strategy of Realization Number 1.

Validation

The results show that the RO strategy leads to an increase in expected NPV and reduced variance against the considered set of realizations. Improved performance of the RO strategy against the

TABLE 2—RESULTS

	Reactive Control	NO (on average)		RO	
Expected NPV	USD 43.7 million	USD 46.3 million	+5.9%	USD 47.9 million	+9.5%
Standard Dev.	USD 1.20 million	USD 1.01 million	–	USD 0.79 million	–

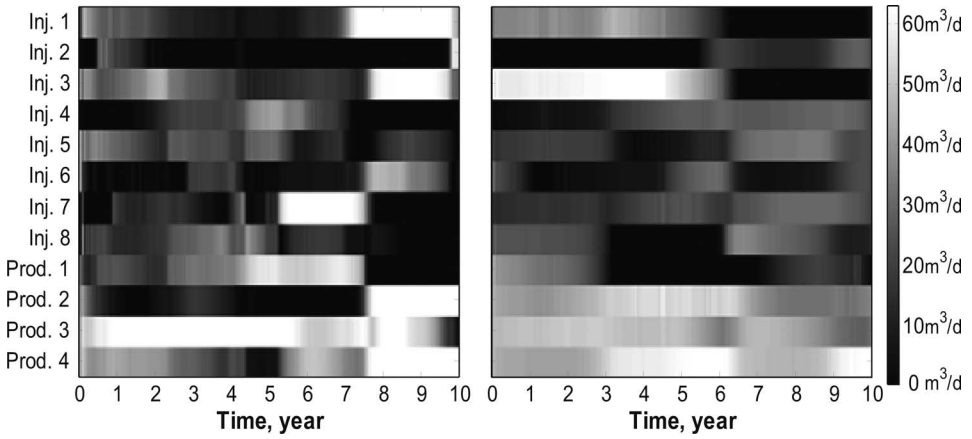

Fig. 5—Injection- and production-flow rates resulting from the NO (left) and the RO (right) of Realization Number 1.

actual underlying geological uncertainty can be claimed only if the set is, in fact, a proper representation of this uncertainty, as was assumed in the introduction of the example. To validate that this assumption is plausible, the different control strategies were checked against the second set of 100 realizations. If both sets are large enough to give a good representation of the range of possible geological structures, the different strategies should lead to similar responses in a statistical sense.

T3 **Table 3** presents the averaged expected NPV and standard deviation of the reactive, NO and RO strategies, applied to this second validation set. F6 **Figs. 6a and 6b** show the estimated PDFs of the reactive control strategy and of the RO control strategy, respectively, applied to the original and the validation set. Figs. 6b and 6c show the PDFs of the NO strategy with the lowest expected NPV and with the highest expected NPV, respectively; Figs 6d and 6e show two intermediate values of expected NPV. Table 3 and Fig. 6 show that the responses of the strategies to the different sets are very similar. This indicates that the assumption of the set being a proper representation of the geological uncertainty is, in fact, plausible.

Remarks

In this work, injection- and production-flow rates are used to manipulate the progression of the oil/water front in the reservoir. The equality constraint, resulting from using flow rates as control variables, limits the search space of the optimization algorithm. Alternatively, the optimization may be performed using bottomhole pressures or control-valve settings as control variables, which would require the use of well-inflow models. In that case, the use of an equality constraint to enforce balanced injection and production would no longer be necessary. Moreover, in this study, no measurement information was assumed to be available. Additional measurement information could be used, however, to reduce the geological uncertainty associated within the reservoir model. In future research on RO of reservoir flooding, a more integrated approach is advised, in which measurements are used to narrow the set of realizations or to improve the quality of the set through history matching.

Conclusions

An RO technique is an attractive approach to oil-recovery-optimization problems because it creates a bridge between two aspects of the E&P industry: geological uncertainty and maximizing oil-recovery revenues. We tested its expected performance against those of NO strategies and reactive strategies by simulating a waterflooding example using 100 realizations of a fluvial reservoir. From the results of the example, we conclude that

- The performance of the NO strategy depends heavily on the particular realization that is selected to base the optimization on. In the example, there is no motivation to regard one geological structure to be more likely than the others, but the results of the resulting NOs are very different and nearly always worse than the result of the RO strategy.
- The RO strategy is able to improve the expected NPV significantly compared to the NO and reactive strategies, and it results in a smaller range of possible NPV outcomes (variance reduction) when tested using the initial set of realizations. The improved performance is maintained when the RO strategy is tested using a second (validation) set of realizations. This indicates that the set of 100 realizations is likely to be a proper representation of the geological uncertainty considered in this example.
- The advantage of a reactive strategy is that it is model-free. Thus, when applied to an actual field, it does not suffer from a wrong representation of the geological realizations, whereas the model-based RO and NO methods do. However, the disadvantage is that it usually does not lead to an optimal reservoir flooding in terms of life-cycle performance.
- It should be stressed that the conclusion of improved performance of the RO strategy compared to those of the NO and reactive strategies holds only if the used set of geological realizations is a good representation of the true modeling uncertainty. If the used set is far from accurate, it is impossible to say which of the considered strategies will perform better.

Nomenclature

b = discount rate
c = compressibility, Lt^2/m, 1/Pa
$\mathbf{d}$ = feasible-direction vector
E = expected-value operator
$\mathbf{F}$ = fractional-flow matrix
$\mathbf{g}$ = system equations
i = iteration counter
J = objective function, M, USD

TABLE 3—VALIDATION

	Reactive Control	NO (on average)	RO
Expected NPV	USD 43.6 million	USD 46.3 million	USD 47.9 million
Standard Dev.	USD 1.24 million	USD 0.93 million	USD 0.73 million

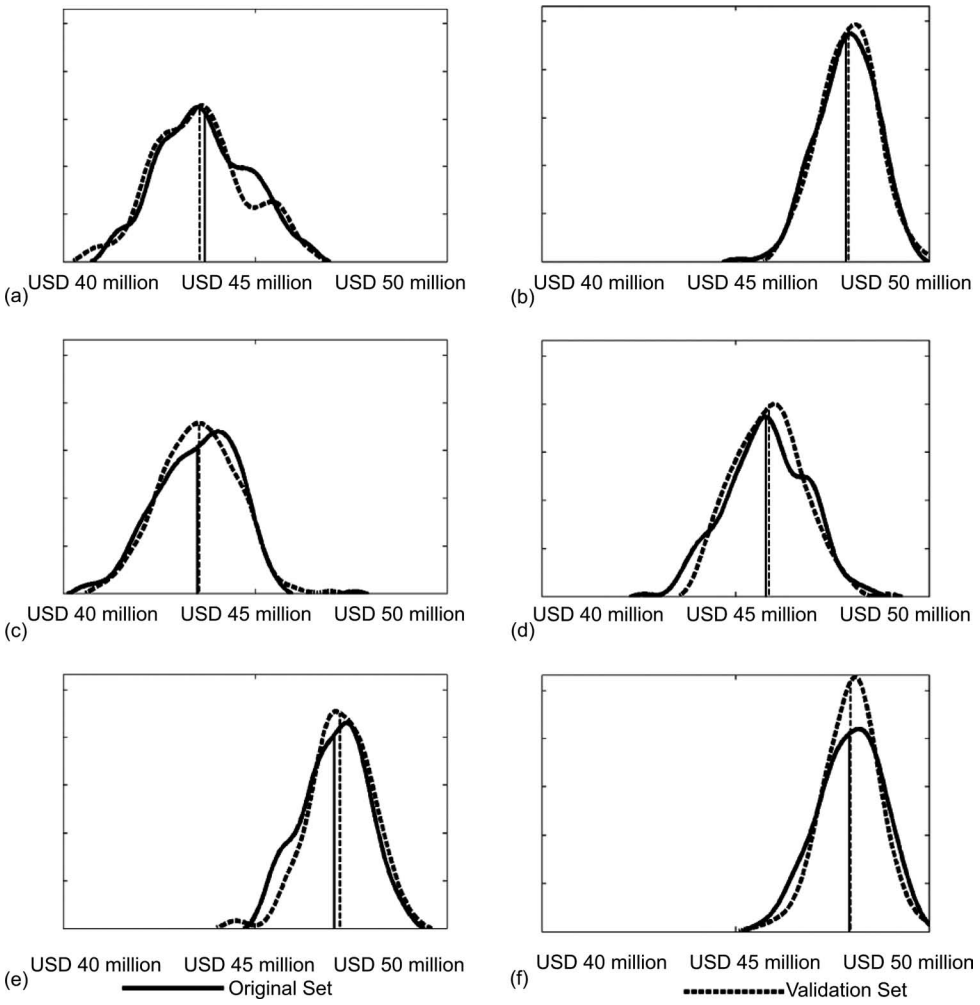

Fig. 6—Estimated PDFs of the reactive control strategy (a), the RO control strategy (b), the NO strategy with the lowest expected NPV (c), the highest expected NPV (f), and two intermediate values of expected NPV (d and e), applied to the original and the validation set of realizations.

$\bar{J}$ = modified objective function, M, USD
k = timestep counter
K = total number of timesteps
N_r = total number of realizations
p = pressure, m/(Lt^2), Pa
$\mathbf{q}$ = vector of flow rates, L^3/t, m^3/s
r = price per unit volume, M/L^3, USD/m^3
t = time, t, seconds
$\mathbf{x}$ = state vector
α = weight factor (step size)
$\boldsymbol{\eta}$ = vector of averages of model parameters
$\boldsymbol{\theta}$ = vector of uncertain model parameters
Θ = uncertainty space
κ = dummy variable in summation
$\boldsymbol{\lambda}$ = Lagrange-multiplier vector
μ = viscosity, m/Lt, Pa·s
ρ = density, m/L^3, kg/m^3
τ = reference time for discounting, t, seconds
ϕ = porosity

Subscripts

cow = oil/water capillary
d = deterministic
max = maximum
min = minimum
o = oil
r = realization
rob = robust
w = water
wp = produced water
wi = injected water

Acknowledgments

This research was carried out within the context of the Integrated Systems Approach to Petroleum Production (ISAPP) knowledge center. ISAPP is a joint project between Delft University of Technology (TUD), Shell International Exploration and Production (SIEP), and the Dutch Organization for Applied Scientific Research (TNO).

References

Aziz, K. and Settari, A. 1979. *Petroleum Reservoir Simulation.* Essex, UK: Elsevier Applied Science Publishers.

Brouwer, D.R. and Jansen, J.-D. 2004. Dynamic Optimization of Water Flooding With Smart Wells Using Optimal Control Theory. *SPEJ* **9** (4): 391–402. SPE-78278-PA. DOI: 10.2118/78278-PA.

Caers, J., Strebelle S., and Payrazyan, K. 2003. Interpreter's Corner—Stochastic integration of seismic data and geologic scenarios: A West Africa submarine channel saga. *The Leading Edge* **22** (3): 192–196. DOI:10.1190/1.1564521.

de Montleau, P., Cominelli, A., Neylon, K., Rowan, D., Pallister, I., Tesaker, O., and Nygard, I. 2006. Production Optimization under Constraints Using Adjoint Gradients. Paper A041 presented at the 10th European Conference on the Mathematics of Oil Recovery, Amsterdam, 4–7 September.

Deutsch, C.V. and Tran, T.T. 2002. FLUVSIM: a program for object-based stochastic modeling of fluvial depositional systems. *Computers & Geosciences* **28** (4): 525–535. DOI:10.1016/S0098-3004(01)00075-9.

Gross, L.J. and Small, M.J. 1998. River and floodplain process simulation for subsurface characterization. *Water Resources Research* **34** (9): 2365–2376. DOI:10.1029/98WR00777.

Jansen, J.D., Brouwer, D.R., Naevdal, G., and van Kruijsdijk, C.P.J.W. 2005. Closed-loop reservoir management. *First Break* **23** (January): 43–48.

Kraaijevanger, J.F.B.M., Egberts, P.J.P., Valstar, J.R., and Buurman, H.W. 2007. Optimal Waterflood Design Using the Adjoint Method. Paper SPE 105764 presented at the SPE Reservoir Simulation Symposium, Houston, 26–28 February. DOI: 10.2118/105764-MS.

Landa, J.L. and Horne, R.N. 1997. A Procedure to Integrate Well Test Data, Reservoir Performance History and 4-D Seismic Information into a Reservoir Description. Paper SPE 38653 presented at the SPE Annual Technical Conference and Exhibition, San Antonio, Texas, USA, 5–8 October. DOI: 10.2118/38653-MS.

Li, R., Reynolds, A.C., and Oliver, D.S. 2003. History matching of three-phase flow production data. *SPEJ* **8** (4): 328–340. SPE-87336-PA. DOI: 10.2118/87336-PA.

Luenberger, D.G. 1984. *Linear and Nonlinear Programming*, second edition. Columbus, Ohio: Addison-Wesley.

Ruppen, D., Benthack, C., and Bonvin, D. 1995. Optimization of batch reactor operation under parametric uncertainty—computational aspects. *Journal of Process Control* **5** (4): 235–240. DOI:10.1016/0959-1524(95)00015-I.

Sarma, P., Aziz, K., and Durlofsky, L.J. 2005. Implementation of Adjoint Solution for Optimal Control of Smart Wells. Paper SPE 92864 presented at the SPE Reservoir Simulation Symposium, The Woodlands, Texas, USA, 31 January–2 February. DOI: 10.2118/92864-MS.

Sarma, P., Chen, W.H., Durlofsky, L.J., and Aziz, K. 2006. Production Optimization With Adjoint Models Under Nonlinear Control-State Path Inequality Constraints. *SPEREE* **11** (2): 326–339. SPE-99959-PA. DOI: 10.2118/99959-PA.

Srinivasan, B., Bonvin, D., Visser, E., and Palanki, S. 2003. Dynamic optimization of batch processes: II. Role of measurements in handling uncertainty. *Computers & Chemical Engineering* **27** (1): 27–44. DOI:10.1016/S0098-1354(02)00117-5.

Strebelle, S. 2000. Sequential simulation drawing structures from training images. PhD thesis, Stanford University, Stanford, California.

Terwiesch, P., Ravemar, D., Schenker, B., and Rippin, D.W.T. 1998. Semi-batch process optimization under uncertainty: Theory and experiments. *Computers & Chemical Engineering* **22** (1–2): 201–213. DOI:10.1016/S0098-1354(96)00359-6.

Thomas, R. and Nicholas, A.P. 2002. Simulation of braided river flow using a new cellular routing scheme. *Geomorphology* **43** (3–4): 179–195. DOI:10.1016/S0169-555X(01)00128-3.

Viseur, S. 1999. Stochastic Boolean Simulation of Fluvial Deposits: A New Approach Combining Accuracy With Efficiency. Paper SPE 56688 presented at the SPE Annual Technical Conference and Exhibition, Houston, 3–6 October. DOI: 10.2118/56688-MS.

Yeten, B., Durlofsky, L.J., and Aziz, K. 2002. Optimization of Smart Well Control. Paper SPE 79031 presented at the SPE International Thermal Operations and Heavy Oil Symposium and International Horizontal Well Technology Conference, Calgary, 4–7 November. DOI: 10.2118/79031-MS.

Appendix A—Gradient Calculation Using a System of Adjoint Equations

We consider the usual equations for multiphase flow through porous media on the basis of conservation of mass and Darcy's law, equations of state and the empirical closure equations for capillary pressure, and relative permeabilities (Aziz and Settari 1979). Using some form of spatial discretization, such as a finite-volume or finite-element method, and an implicit time discretization, we obtain discrete-time system equations that can be expressed as

$$\mathbf{g}_{k+1}(\mathbf{u}_{k+1}, \mathbf{x}_{k+1}, \mathbf{x}_k) = \mathbf{0}, \quad \text{(A-1)}$$

where $\mathbf{g}$ is a vector-valued function and $\mathbf{x}$ is the state vector containing pressures and phase saturations (or component accumulations) in each gridblock (i.e., finite volume or finite element). In general, the input vector $\mathbf{u}$ contains well flow rates, well pressures, or valve settings in those gridblocks that are penetrated by wells. In this paper, we restrict the input variables to total flow rates. Therefore, we can write

$$\mathbf{g}_{k+1}(\mathbf{q}_{k+1}, \mathbf{x}_{k+1}, \mathbf{x}_k) = 0. \quad \text{(A-2)}$$

To complete the model, we specify the initial conditions

$$\mathbf{x}_0 = \breve{\mathbf{x}}_0. \quad \text{(A-3)}$$

Next, we consider the flooding-optimization problem

$$\max_{\mathbf{q}_{1:K}} J(\mathbf{q}_{1:K}), \quad \text{(A-4)}$$

with objective function

$$J(\mathbf{q}_{1:K}) = \sum_{k=1}^{K} J_k(\mathbf{q}_{1:k}), \quad \text{(A-5)}$$

where J_k represents the contribution to J in each timestep as defined in more detail in Eq. 1. Note that we could formally write Eq. A-5 as

$$J(\mathbf{q}_{1:K}) = \sum_{k=1}^{K} J_k(\mathbf{q}_k(\mathbf{x}_k(\mathbf{q}_{1:k}))) \quad \text{(A-6)}$$

to reflect the dependence on earlier inputs through the recurrence relationship (Eq. A-1), but we will refrain from doing so to keep the notation tractable. The injection and production rates are subject to inequality constraints as they are bounded by a minimum ($\mathbf{q}_{\min}$) and maximum ($\mathbf{q}_{\max}$) rate. An additional equality constraint is required stating that the total water-injection rate $\mathbf{q}_{wi}$ must equal the negative of the total production rate ($\mathbf{q}_o + \mathbf{q}_{wp}$) at each timestep k, such that reservoir pressure remains constant:

$$\mathbf{q}_{\min} \le \mathbf{q}_k \le \mathbf{q}_{\max} \quad \text{(A-7)}$$

and

$$\mathbf{q}_{o,k} + \mathbf{q}_{wp,k} = -\mathbf{q}_{wi,k}. \quad \text{(A-8)}$$

The optimization problem can now be formulated as finding the input vector $\mathbf{q}_k$ that maximizes J over the time interval $k = 1, \ldots, K$, subject to system Eq. A-2, initial conditions Eq. A-3, and constraints Eqs. A-7 and A-8. We aim to compute the optimal control $\mathbf{q}_{1:K}$ with the aid of a gradient-based algorithm, which requires the derivatives of J with respect to $\mathbf{q}_{1:K}$. The complex dependence of J on $\mathbf{q}_{1:K}$ can be taken into account by considering Eqs. A-2 and A-3 as additional constraints to the optimization problem, and applying the technique of Lagrange multipliers to solve the constrained optimization problem:

$$\bar{J}(\mathbf{q}_{0:K}, \mathbf{x}_{0:K}, \lambda_{0:K}) = \sum_{k=0}^{K-1} \begin{bmatrix} J_{k+1}(\mathbf{q}_{1:k+1}) + \lambda_0^T (\mathbf{x}_0 - \breve{\mathbf{x}}_0) \delta_k \\ + \lambda_{k+1}^T \mathbf{g}_{k+1}(\mathbf{q}_{k+1}, \mathbf{x}_k, \mathbf{x}_{k+1}) \end{bmatrix}, \quad \text{(A-9)}$$

where the constraints have been adjoined to J with the aid of vectors of Lagrange multipliers $\boldsymbol{\lambda}$. The Kronecker delta δ_k ensures that the initial-condition constraint is included in the summation. We note that the ordinary constraints Eqs. A-7 and A-8 are not included in this formulation because they are taken care of with the aid of the gradient projection method, as described in the body of the text. We can obtain a first-order description $\partial\bar{J}/\partial\mathbf{q}_k$ of the

effect of changing $\mathbf{q}_k$ on the magnitude of $\bar{J}$ through taking the first variation of Eq. A-9. A necessary condition for an optimum is stationarity of $\bar{J}$ for all variations, which leads to the following set of equations:

$$\frac{\partial J_{k+1}}{\partial \mathbf{q}_{k+1}} + \lambda_{k+1}^T \frac{\partial \mathbf{g}_{k+1}}{\partial \mathbf{q}_{k+1}} = \mathbf{0}^T, \qquad \text{(A-10)}$$

$$\lambda_1^T \frac{\partial \mathbf{g}_1}{\partial \mathbf{x}_0} + \lambda_0^T = \mathbf{0}^T, \qquad \text{(A-11)}$$

$$\lambda_{k+1}^T \frac{\partial \mathbf{g}_{k+1}}{\partial \mathbf{x}_k} + \lambda_k^T \frac{\partial \mathbf{g}_k}{\partial \mathbf{x}_k} = \mathbf{0}^T, \qquad \text{(A-12)}$$

$$\lambda_K^T \frac{\partial \mathbf{g}_K}{\partial \mathbf{x}_K} = \mathbf{0}^T, \qquad \text{(A-13)}$$

$$\left(\mathbf{x}_0 - \breve{\mathbf{x}}_0\right)^T = \mathbf{0}^T, \qquad \text{(A-14)}$$

and

$$\mathbf{g}^T(\mathbf{q}_{k+1}, \mathbf{x}_k, \mathbf{x}_{k+1}) = \mathbf{0}^T. \qquad \text{(A-15)}$$

The last two equations are identical to system equation Eq. A-2 and initial-condition equation Eq. A-3 and are, therefore, automatically satisfied. Eq. A-13 reveals that the Lagrange-multiplier vector λ_K for the final discrete time K is equal to 0, and the discrete-time differential equation Eq. A-12 allows us to recursively compute the multipliers λ_K for $k = K-1, \ldots, 0$ (i.e., backward in time). Eq. A-11 represents the effect of changing the initial condition $\mathbf{x}_0$ on the value of the objective function, while keeping all other variables fixed. However, because we prescribed the initial condition through Eq. A-3, in our case, this term is of theoretical relevance only. Finally, Eq. A-10 represents the effect of changing the control on the value of the objective function while keeping all other variables fixed. For a nonoptimal control, this term is not equal to zero, but then its residual is just the gradient that we require to obtain iteratively the optimal control using a gradient-based algorithm. Solution of the optimization problem now consists of choosing an initial control vector $\mathbf{q}_{1:K}$ and repeating the following steps until the optimal control vector $\mathbf{q}_{1:K}$ has been found:

- Compute the states $\mathbf{x}_{1:K}$ using Eq. A-2, starting from initial-conditions equation Eq. A-3.
- Compute the value of the objective function J using Eq. A-5. If converged, stop; otherwise continue.
- Compute the Lagrange multipliers $\lambda_{1:K}$ using Eqs. A-13 and A-12.
- Compute the derivatives (transposed gradients) of the objective function to the controls from the residuals of Eq. A-10 according to:

$$\frac{\mathrm{d}J}{\mathrm{d}\mathbf{q}_{k+1}} = \frac{\partial \bar{J}}{\partial \mathbf{q}_{k+1}} = \frac{\partial J_{k+1}}{\partial \mathbf{q}_{k+1}} + \lambda_{k+1}^T \frac{\partial \mathbf{g}_{k+1}}{\partial \mathbf{q}_{k+1}}. \qquad \text{(A-16)}$$

- Compute an improved estimate of the control vector $\mathbf{q}_{1:K}$, using the derivatives as obtained from Eq. A-16 and a gradient-based minimization routine of choice (e.g., the SA method as described in Eq. 3).

Because of its computational efficiency in calculating the gradients of the objective function, adjoint-based optimization is particularly attractive for problems with a large number of control parameters.

Gijs van Essen is a PhD student at Delft University of Technology who works on production optimization and reservoir management. email: g.m.vanessen@tudelft.nl. He holds an MS degree in systems and control from Delft University of Technology. **Maarten Zandvliet** is a reservoir engineer with Shell International Exploration & Production. email: maarten.zandvliet@shell.com. He has worked with Shell in The Netherlands since 2008 in well and reservoir management. He holds MS and PhD degrees from Delft University of Technology. **Paul Van den Hof** is professor and codirector of the Delft Center for Systems and Control. email: p.m.j.vandenhof@tudelft.nl. He holds MS and PhD degrees from the Department of Electrical Engineering, Eindhoven University of Technology. Van den Hof's research interests are in issues of system identification, parameterization, signal processing, and (robust) control design. **Okko Bosgra** holds an MS degree in mechanical engineering from Delft University of Technology. email: o.h.bosgra@tue.nl. Since 1986, he has been a professor in control engineering, heading the Mechanical Engineering Systems and Control Group of Delft University of Technology. Since 2003, he has also been a part-time professor in the Control Systems Technology Group of the Mechanical Engineering Department of Eindhoven University of Technology. **Jan-Dirk Jansen** has a split assignment as professor of reservoir systems and control at Delft University of Technology and as consultant in the Improved and Enhanced Oil Recovery Program of Shell International Exploration & Production. e-mail: j.d.jansen@tudelft.nl. He has worked with Shell since 1986 in research and operations in The Netherlands, Norway, and Nigeria. He holds MS and PhD degrees from Delft University of Technology.